

Supporting Information

Characterization

Using X-ray diffraction (XRD) to ascertain the crystal phase of composition at 10° to 80° by Bruker D8 diffractometer. The surface morphology and internal crystal structure of samples were observed by SEM (Hitachi 8100) and TEM (FEI F20 S-TWIN). The thermogravimetric analysis (TGA) was conducted to measure the compound by TA-SDT Q600 analyzer. The heating rate in the atmosphere was $10^\circ\text{C min}^{-1}$. The attribute of chemical bonds was determined by Raman spectroscopy (DXR2xi) of a 532 nm laser. The surface property of the composition was researched by X-ray photoelectron spectroscopy (XPS).

Electrochemical measurements

For SIBs, the anode electrode was formed by blending the active component, super P and carboxymethyl cellulose (CMC) in a proportion of 8: 1: 1 in deionized water. Each active material loaded in the anode electrodes is closed to $1.5\text{-}2.5\text{ mg cm}^{-2}$ for SIBs tests system. The solution was fixed to copper foil and dried at 80°C overnight under vacuum. In the half sodium-ion batteries, 1 M NaClO_4 in 1:1 (weight ratio) EC/DMC with 5% fluoroethylene carbonate (FEC) additives and whatman glass fiber were conducted as electrolyte and separator, respectively. In the half-cells, sodium metal was served as the counter electrode. For full SIBs, the capacity ratio of WS_2 -SPAN-2 anode and NVP cathode was optimized to 1: 1.2. The WS_2 -SPAN-2 anode was pre-cycled for three times before assembling full cells and before measuring the high and low temperature performance.

As for PIBs half-battery, the anode was fabricated by admixing the active materials (WS_2 -SPAN-2, 80 wt.%) with super P (10 wt.%) and CMC (10 wt.%) in deionized water. Every active material loaded in active materials in the anode electrodes is closed to $1.5\text{-}2.5\text{ mg cm}^{-2}$ for PIBs tests. In addition, 3.0 M potassium bis(fluorosulfonyl)imide (KFSI) in DME (100% Vol%) was employed as electrolyte. The counter electrode was made up of sheet potassium metal. Notably, all the assembly work was carried out in a glove box filled with high pure argon.

Electrochemical characterization

Galvanostatic charge/discharge tests and the galvanostatic intermittent titration technique (GITT) of the electrode materials were tested on Land CT 2001A tester between 0.01 to 3 V. The cyclic voltammetry (CV) tests were conducted by an Ivium-n-Stat electrochemical workstation at diverse scan rates (vs. Na/Na^+ or K/K^+).

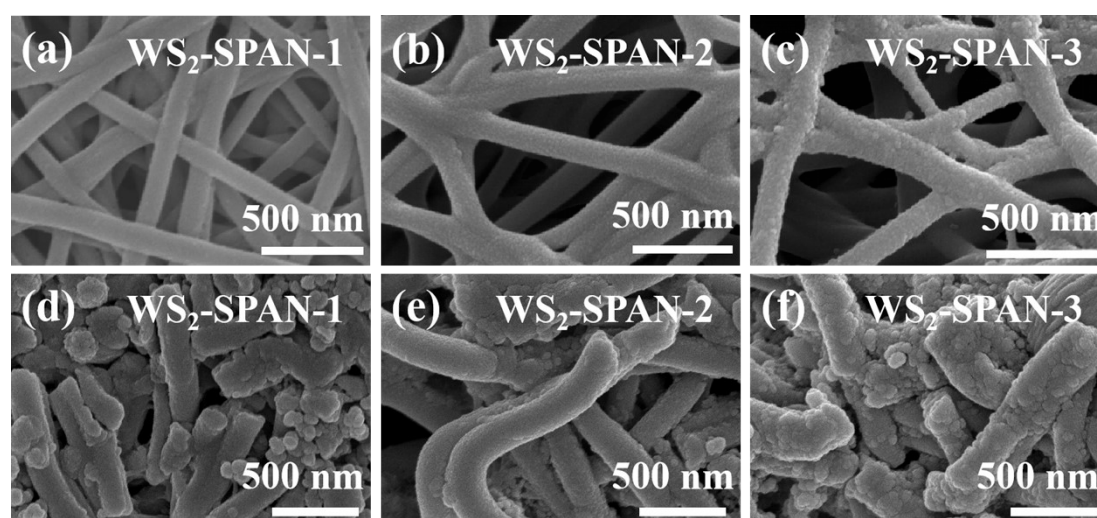


Fig. S1 SEM images before (a-c) and after cycling (d-f) of WS_2 -SPAN-1, WS_2 -SPAN-2 and WS_2 -SPAN-3 electrodes.

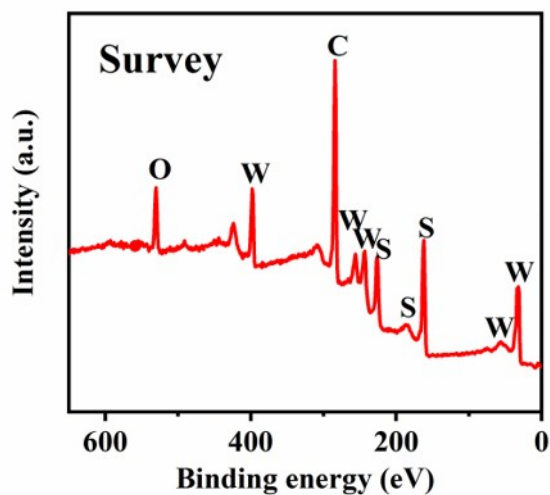


Fig. S2 Survey spectrum of WS₂-SPAN-2 sample.

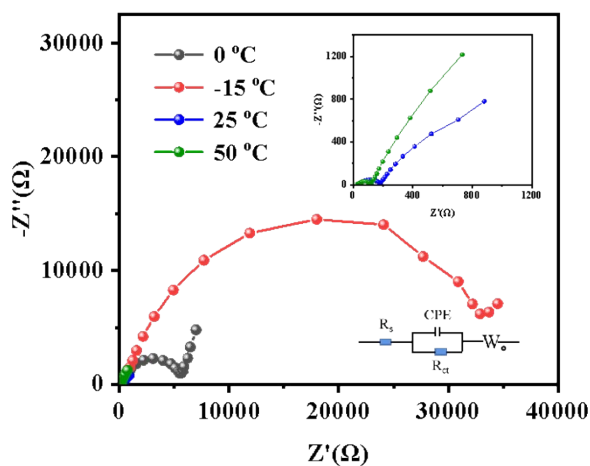


Fig. S3 Electrochemical impedance spectra (EIS) of WS₂-SPAN-2 electrodes at different temperatures in SIBs.

Table S1 Impedance values fitted from an equivalent circuit model.

Temperature	R _s (Ω)	R _{ct} (Ω)
-15 °C	139.8	42294
0 °C	74.5	6875
25 °C	30.8	170.3
50 °C	23.7	122.9

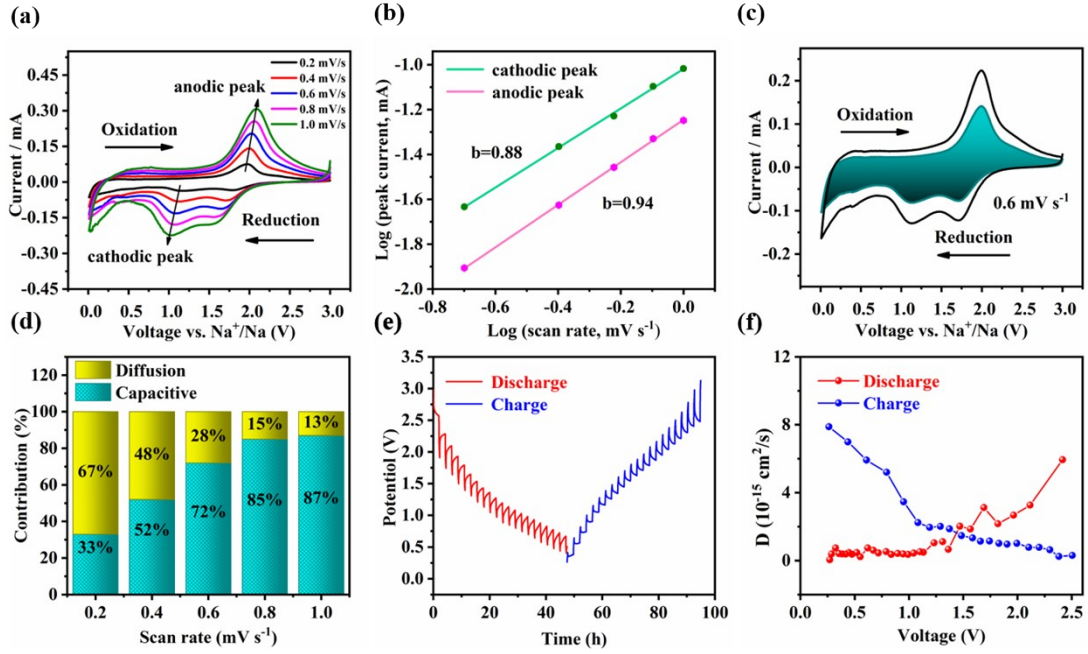


Fig. S4 (a) Cyclic voltammety curves of WS₂-SPAN-2 electrode at different scan rates from 0.2 to 1.0 mV·s⁻¹. (b) log (i) versus log (v) plots at different oxidation and reduction peaks. (c) Capacitive contribution (green area) of WS₂-SPAN-2 at 0.6 mV·s⁻¹. (d) The diffusion controlled (yellow) and capacitive (blue) capacities of WS₂-SPAN-2 at different scan rates. (e) GITT charge/discharge profile, (f) Na⁺ diffusion coefficients and reaction resistance for the WS₂-SPAN-2 anode of SIBs.

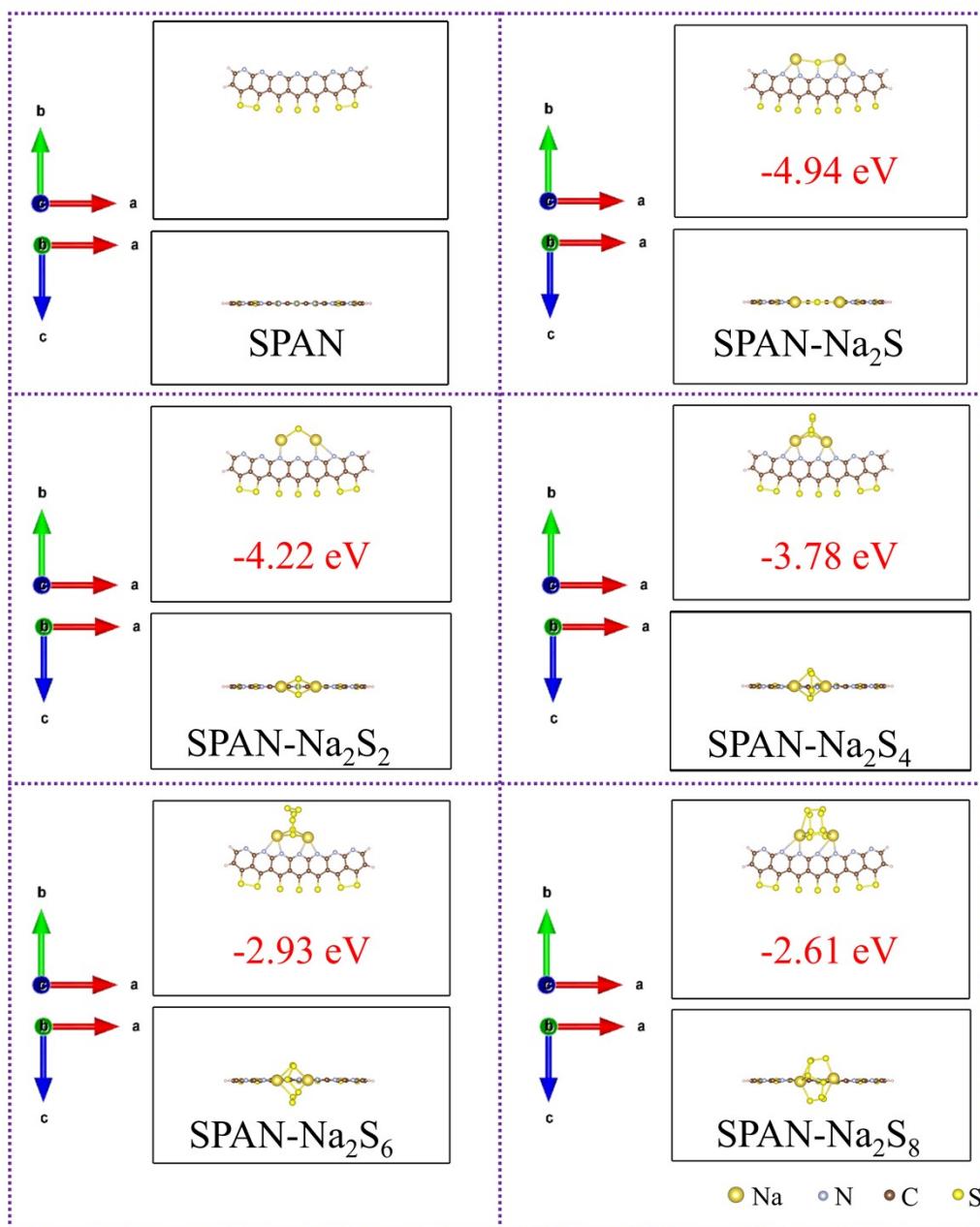


Fig. S5 Front and top views of optimized configurations of sodium polysulfide Na_2S_n ($n=1, 2, 4, 6$ and 8) clusters adsorbed on SPAN.

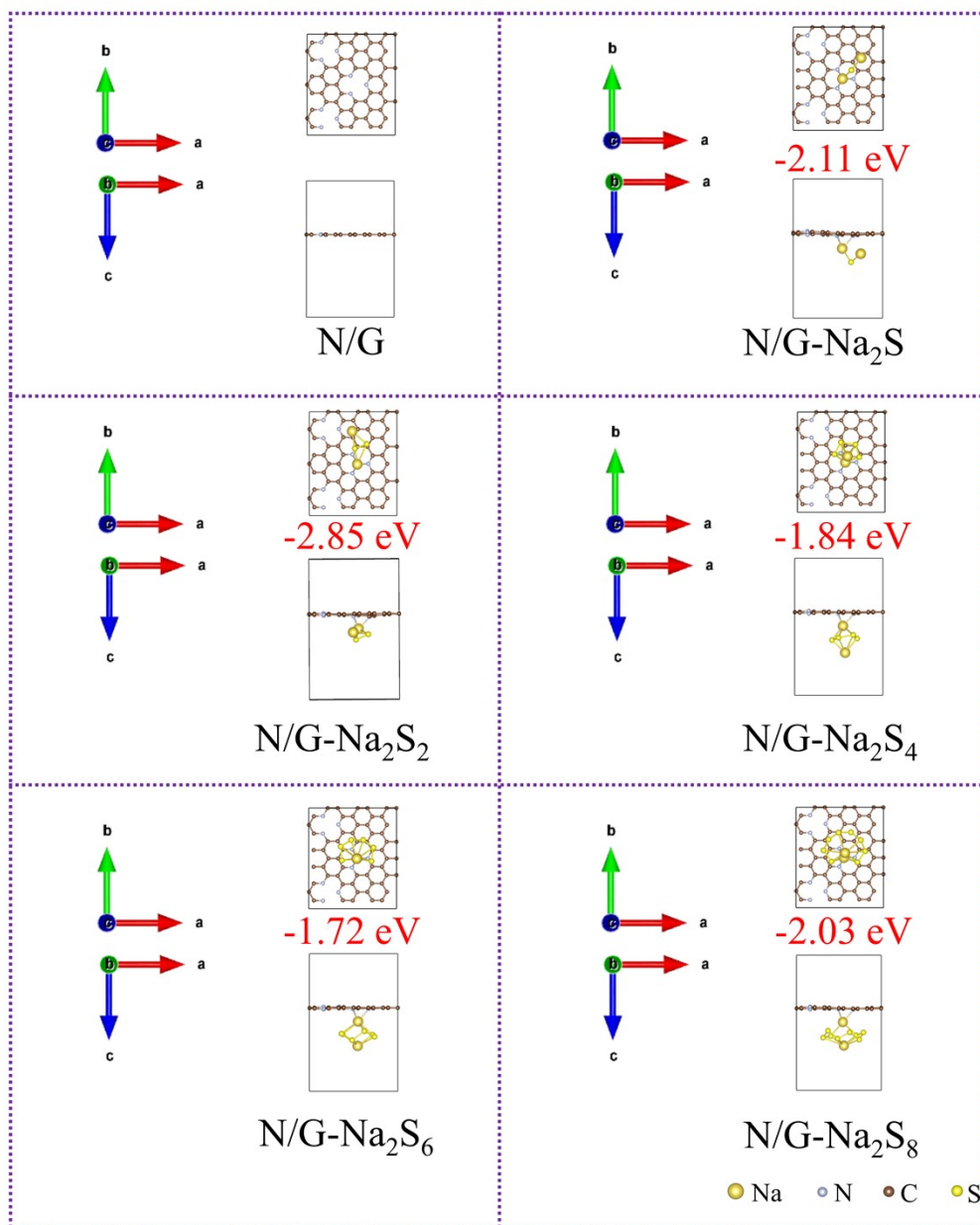


Fig. S6 Front and top views of optimized configurations of sodium polysulfide Na_2S_n ($n = 1, 2, 4, 6$ and 8) clusters adsorbed on N/G.

Table S2 Cycling performance of the WS₂-SPAN-2 electrode and newly reported WS₂ based and other anodes for SIBs/PIBs.

Electrode materials	fields	Cycling capacity (mAh g ⁻¹)	Current density (A g ⁻¹)	Cycle numbers	Ref.
WS ₂ -SPAN-2	SIBs	464	0.5	450	This work
		354	2	1400	
		190	5	12000	
		129	10	18000	
WS ₂ -SPAN-2	-15 °C	307/210	0.5/1	200/500	This work
	0 °C	402/266			
	25 °C	457/382			
	50 °C	245/228			
WS ₂ -SPAN-2	PIBs	362	0.1	100	This work
		278	1	3000	
WS ₂	SIBs	471	0.2	300	3
		240	5	250	
WS ₂ @NC	SIBs	384	1	200	11
		151	5	500	
H-WS ₂ @NC	SIBs	468	0.1	200	14
		375	1	1000	
WS ₂ /CNT-rGO	SIBs	311	0.1	100	18
		252	0.2	100	
Co ₉ S ₈ /WS ₂ @N C	SIBs	405	1	100	25
		354	2	120	
FeSe ₂ /rGO	-40 °C	217	1	200	37
	60 °C	422	5		
WS ₂ @S/N-C	SIBs	321	0.1	100	44
		175	5	1000	
C-WS ₂ @CNFs	PIBs	247	0.5	300	61
		168	2		
WS ₂ @rGO-HC	SIBs	522	0.1	70	S1
		190	1	200	
WS ₂	PIBs	103	0.1	100	S2
FeS ₂ /WS ₂ - CNFs	SIBs	423	0.5	500	S3
		308	4	1000	
WS ₂ hollow spheres	SIBs	353	0.2	80	S4
		285	2	2000	

WS ₂ -MWCNTs	SIBs	289	1	60	S5
NGQDs- WS ₂ /3DCF	SIBs	268	2	1000	S6
HB WS ₂ @CNFs	SIBs	381 130	0.2 2	100 300	S7

Refs:

- [S1] J. Li, X. Shi, J. Fang, J. Li and Z. Zhang, Facile synthesis of WS₂ nanosheets-carbon composites anodes for sodium and lithium ion batteries, *ChemNanoMat*, 2016, **2**, 997-1002.
- [S2] Y. Wu, Y. Xu, Y. Li, P. Lyu, J. Wen, C. Zhang, M. Zhou, Y. Fang, H. Zhao U. Kaiser and Y. Lei, Unexpected intercalation-dominated potassium storage in WS₂ as a potassium-ion battery anode, *Nano Res.*, 2019, **12**, 2997-3002.
- [S3] H. Wu, N. Xu, Z. Jiang, A. Zheng, Q. Shi, R. Lv, L. Ni, G. Diao and M. Chen, Space and interface confinement effect of necklace-box structural FeS₂/WS₂ carbon nanofibers to enhance Na⁺ storage performance and electrochemical kinetics, *Chem. Eng. J.*, 2022, **427**, 131002.
- [S4] J. Wang, L. Yu, Z. Zhou, L. Zeng and M. Wei, Template-free synthesis of metallic WS₂ hollow microspheres as an anode for the sodium-ion battery, *J. Colloid Interface Sci.*, 2019, **557**, 722-728.
- [S5] X. Li, J. Zhang, Z. Liu, C. Fu and C. Niu, WS₂ nanoflowers on carbon nanotube vines with enhanced electrochemical performances for lithium and sodium-ion batteries, *J. Alloys Compd.*, 2018, **766**, 656-662.
- [S6] Y. Wang, D. Kong, S. Huang, Y. Shi, M. Ding, Y. Von Lim, T. Xu, F. Chen, X. Li and H.Y. Yang, 3D carbon foam-supported WS₂ nanosheets for cable-shaped flexible sodium ion batteries, *J. Mater. Chem. A*, 2018, **6**, 10813-10824.
- [S7] H. Wu, X. Chen, C. Qian, H. Yan, C. Yan, N. Xu, Y. Piao, G. Diao and M. Chen, Confinement growth of layered WS₂ in hollow beaded carbon nanofibers with synergistic anchoring effect to reinforce Li⁺/Na⁺ storage performance, *Small*, 2020, **16**, 2000695.